ELSEVIER

Polymer 44 (2003) 1067–1074

polymer

www.elsevier.com/locate/polymer

Miscibility and intermolecular specific interactions in blends of poly(hydroxyether of bisphenol A) and poly(4-vinyl pyridine)

Sixun Zheng[a,b], Yongli Mi[a,*]

[a]*Department of Chemical Engineering, The Hong Kong University of Science and Technology, Clear Water Bay, Kowloon, Hong Kong, People's Republic of China*

[b]*Department of Polymer Science and Engineering, Shanghai Jiao Tong University, Shanghai 200240, People's Republic of China.*

Received 15 August 2002; received in revised form 13 November 2002; accepted 19 November 2002

Abstract

The blends of poly(hydroxyether of bisphenol A) (phenoxy) with poly(4-vinyl pyridine) (P4VPy) were investigated by differential scanning calorimetry (DSC), Fourier transform infrared spectroscopy (FTIR) and high-resolution solid-state nuclear magnetic resonance (NMR) spectroscopy. The single, composition-dependent glass transition temperature (T_g) was observed for each blend, indicating that the system is completely miscible. The sigmoid T_g-composition relationship is characteristic of the presence of the strong intermolecular specific interactions in the blend system. FTIR studies revealed that there was intermolecular hydrogen bonding in the blends and the intermolecular hydrogen bonding between the pendant hydroxyl groups of phenoxy and nitrogen atoms of pyridine ring is much stronger than that of self-association in phenoxy. To examine the miscibility of the system at the molecular level, the high resolution ^{13}C cross-polarization (CP)/magic angle spinning (MAS) together with the high-power dipolar decoupling (DD) NMR technique was employed. Upon adding P4VPy to the system, the chemical shift of the hydroxyl-substituted methylene carbon resonance of phenoxy was observed to shift downfield in the ^{13}C CP/MAS spectra. The proton spin–lattice relaxation time $T_1(H)$ and the proton spin–lattice relaxation time in the rotating frame $T_{1\rho}(H)$ were measured as a function of the blend composition. In light of the proton spin–lattice relaxation parameters, it is concluded that the phenoxy and P4VPy chains are intimately mixed on the scale of 20–30 Å.

Keywords: Poly(hydroxyether of bisphenol A); Poly(4-vinylpyridine); Miscibility

1. Introduction

Polymer blends have been of importance in the engineering industry in the past decades. Thermodynamically, the miscibility of polymer blends is mainly dependent on the mixing enthalpy because the contribution of the combinatorial entropy to the free energy of mixing is negligibly small, and thus the miscibility of most polymer pairs found so far is caused by intermolecular specific interactions. A better understanding of miscibility and phase behavior of polymer blends is essential for the development of blend materials. A variety of techniques can be employed to investigate the miscibility and phase behavior of polymer blends; e.g. thermal and mechanical analyses, microscopy, light scattering and spectroscopy methods are frequently utilized. The sensitivity of various experimental probes to dimensional scale of the homogeneity spans many orders of magnitude [1,2]. For instance, the behavior of single glass transition for polymer blends purports the homogeneity of the blend system on the scale of 20–30 nm in terms of T_g feature [1–3]. Among spectroscopic techniques, Fourier transform infrared spectroscopy (FTIR) and high-resolution solid-state nuclear magnetic resonance (NMR) spectroscopy have proven to be powerful for investigating the intermolecular specific interactions and the phase behavior of polymer blends. In FTIR approach, the information on the intermolecular interactions in blends can be detected through the variation of relative spectroscopic vibration bands [4]. Solid-state NMR spectroscopy can provide the insight of the homogeneity of polymer blends at the segmental scale. The ^{13}C chemical shifts and/or line shapes of carbon resonance in cross-polarization (CP)/magic angle spinning (MAS) spectra identify the chemical environment of carbon nucleus in the blends and thus their changes

* Corresponding author. Fax: +852-358-0054.
E-mail address: keymix@usthk.ust.hk (Y. Mi).

0032-3861/03/$ - see front matter © 2002 Elsevier Science Ltd. All rights reserved.
PII: S0032-3861(02)00878-9

usually reflect the intermolecular interactions between the blend components. In addition, and perhaps more importantly, the relaxation time measurements of NMR can be employed to examine the scale of miscibility of polymer blends. Dynamic relaxation time of proton in the rotating frame, $T_{1\rho}$(H), of a multi-component system is strongly dependent on the short range (ca. 1 nm) spatial proximity or the mixing of various components since the effect of spin diffusion on T_1(H) and $T_{1\rho}$(H) relaxation can reveal the way in which an efficiently relaxing entity can relax other entities in the polymer blend system. Therefore, it is possible to evaluate the scale of miscibility of polymer blends according to the dynamic NMR relaxation measurement, and this approach is considered to be an NMR criterion for miscibility in polymer blend systems [5–24].

The polymer blends composed of poly(hydroxyether of bisphenol A) (phenoxy) and poly(4-vinyl pyridine) (P4VPy) have been previously studied by Ilarduya et al. by means of differential scanning calorimetry (DSC) and FTIR [25]. This system was recognized to be miscible in terms of the behavior of single glass transition temperatures (T_gs). The early studies reported to evaluate the miscibility on the scale of 10–30 nm in terms of the replacement of T_g features characteristics of component polymers [3], however, the homogeneity of the blends at the molecular level has not been studied. In this communication, we present our studies on the polymer blends by means of DSC, FTIR and ^{13}C CP/MAS NMR spectroscopy. The objective is to acquire an insight of the microstructure of the blends at the molecular level. First, the blend system was re-investigated by DSC to examine the miscibility on the scale of 20–30 nm. Thereafter, FTIR and high-resolution solid-state NMR spectroscopy were used to characterize the intermolecular specific interactions between the two components. The information of phase structure at the molecular level was obtained through the nuclear magnetization relaxation experiment. The ^{13}C CP/MAS/high-power dipolar decoupling (DD) spectra were obtained, and the spin–lattice relaxation time in the laboratory frame (T_1 (H)) and in the rotating frame ($T_{1\rho}$(H)) were measured from solid-state ^{13}C NMR spectroscopy. The spatial dimensions of the microstructures of the polymer blends were estimated in terms of indirect spin diffusion process.

2. Experimental

2.1. Materials and preparation of samples

Poly(hydroxyether of bisphenol A) (phenoxy) used in this study was home synthesized; it has a molecular weight of $M_n = 31{,}500$ and $M_w = 50{,}400$ as measured by GPC relative to polystyrene standard. Poly(*N*-vinyl pyrrolidine) (P4VPy) was purchased from Polysciences Inc, Warrington, PA, USA with a quoted number average molecular weight (M_n) of 150,000–200,000. Prior to use, P4VPy was dried in a vacuum oven at 80 °C for 48 h in order to remove the moisture. Phenoxy/P4VPy blends were prepared by solution casting from chloroform at room temperature, and the majority of the solvent was slowly evaporated at the ambient temperature. To remove the residual solvent, all the blend films obtained were desiccated in vacuo at 60 °C for 2 weeks.

2.2. Measurements

2.2.1. Differential scanning calorimetry (DSC)

The calorimetric measurements were performed on a Perkin–Elmer Pyris 1 differential scanning calorimeter in a dry nitrogen atmosphere. The instrument was calibrated with a standard Indium. In order to measure glass transition temperatures, all the samples (about 10 mg in weight) were first heated up to 190 °C and held for 5 min to remove the thermal history, followed by quenching to −40 °C. A heating rate of 20 °C/min was used in all measurements. Glass transition temperature (T_g) was taken as the midpoint of the heat capacity change.

2.2.2. Fourier transform infrared spectroscopy (FTIR)

FTIR measurements were performed on a Nicolet 750 Fourier transform infrared spectrometer. The chloroform solutions (5 wt%) of phenoxy, P4Vpy, and their blends were casting onto KBr window. The majority of solvent was evaporated at room temperature and the residual solvent was removed in vacuo at 60 °C for 48 h. The films of blends used in the study were sufficiently thin to be within a range where the Beer–Lambert law is obeyed. The spectra were obtained at the resolution of 2 cm^{-1} and of 64 scans.

2.2.3. High-resolution solid-state NMR

High-resolution solid-state NMR experiments were carried out at ambient temperature (27 °C) on a Jeol JNM-EX400 FT NMR spectrometer at the resonance frequencies of 399.65 MHz for proton and 100.40 MHz for carbon-13. The high-resolution ^{13}C NMR spectra were obtained using the CP/MAS together with the high-power DD technique. The 90°-pulse width of 5.5 μs was employed with free induction decay (FID) signal accumulation, and the CP Hartmann–Hahn contact time was set at 1.0 ms for all experiments. The rate of MAS was 5.1–5.6 KHz for measuring ^{13}C spectra and relaxation time. The Hartmann–Hahn CP matching and DD field was 40 KHz. The chemical shifts of all ^{13}C spectra were determined by taking the carbon of solid adamantane (29.5 ppm relative to TMS) as an external reference standard.

The proton spin–lattice relaxation time in the laboratory frame, T_1 (H), was measured by monitoring the decay of specific carbon resonance intensities after $\pi - \tau - \pi/2$ inversion-recovery pulse sequence followed by the cross-polarization. The pulse sequences are shown in Fig. 1(a). Proton spin–lattice relaxation time in the rotating frame $T_{1\rho}$(H) was determined by observing the carbon signal

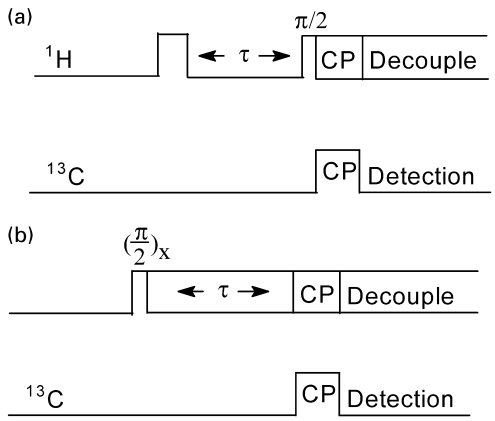

Fig. 1. The pulse sequences used in this work: (a) T_1(H) measurement; (b) $T_{1\rho}$(H) measurement.

intensities with a ^{1}H matched spin-lock-τ pulse sequence prior to CP (Fig. 1(b)).

3. Results and discussion

3.1. Differential scanning calorimetry (DSC)

All the solution-casting films of the blends were transparent at room temperature and the transparency was preserved up to the temperature of 280 °C, at which P4VPy undergoes thermal degradation. This observation suggests that the blends are miscible and no phase separation occurs at least on the scale exceeding the wavelength of visible light. All the phenoxy/P4VPy blends were subjected to DSC measurement and the DSC curves are shown in Fig. 2. It can be seen that, each blend displayed a single glass transition temperature (T_g), intermediate between those of the two pure components and varying with the blend composition. Therefore, it is judged that phenoxy/P4VPy blends are completely miscible over the entire composition range. The T_g values of the blends were plotted as a function of composition in Fig. 3. It is seen that the T_gs of the blends at low P4VPy content show the positive deviation, whereas, at higher P4VPy content, negative deviation is demonstrated. The sigmoid T_g–composition relationship is thus found. This observation is different from the results of weight-average glass transition temperatures reported by Ilarduya et al. [25]. The appearance of the sigmoid T_g–composition behavior is indicative of strong intermolecular interaction between the polymer components. Dependence of T_g on the composition of the miscible polymer blends can be correlated with several empirical equations [26–30]. One of such equations, Gordon–Taylor equation, has been extensively employed to predict the thermal behavior of miscible polymer blends [26]:

$$T_g = ((W_1 T_{g1} + kW_2 T_{g2})/(W_1 + kW_2)) \quad (1)$$

where T_g is the glass transition temperature of the blends,

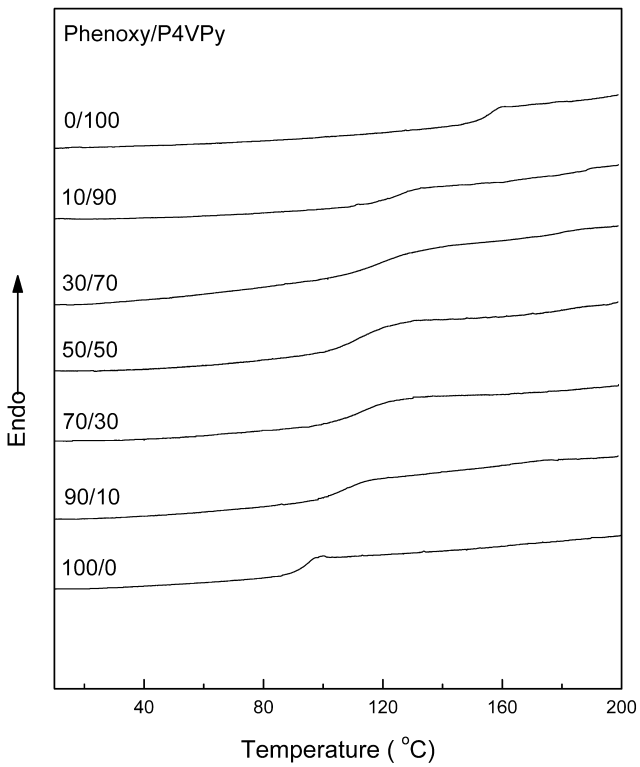

Fig. 2. DSC curves of phenoxy/P4VPy blends.

and T_{g1} and T_{g2} are those of pure components. k is an adjustable fitting parameter, which can be taken as a quantity characterizing the strength of intermolecular interactions. W is the weight fraction. For systems with intermolecular specific interactions, the Kwei equation, which can be taken as a modified Gordon–Taylor equation,

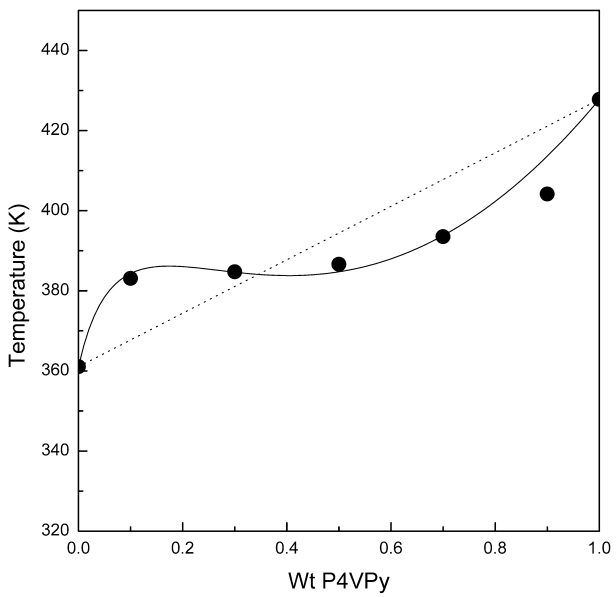

Fig. 3. Plot of glass transition temperature for phenoxy/P4VPy blends as a function of *weight* fraction of P4VPy. (●) T_g; (- - -) the prediction of Kwei equation with $K = 11.1$ and $q = -153.1$.

can well depict the T_g–composition relationship [29,30]:

$$T_g = ((W_1 T_{g1} + kW_2 T_{g2})/(W_1 + kW_2) + qW_1 W_2 \quad (2)$$

The first term on the right hand side of Eq. (2) is identical to Gordon–Taylor equation, which represents the mixing term derived from the additive rule of entropy and/or of the volume of the blends. The quadratic term (qW_1W_2) accounts for intermolecular specific interactions in the mixture. When this equation was applied to fit the experimentally obtained T_gs of the phenoxy/P4VPy blends, the values of $k = 11.05$ and $q = -153.1$ were obtained, indicating strong intermolecular interactions existing between the two components.

3.2. Fourier transform infrared spectroscopy (FTIR)

Poly(4-vinyl pyridine) (P4VPy) shows a marked basic Lewis character: the nitrogen atom incorporated with the side aromatic ring is amenable to share a free electron pair with Lewis acids, which endows the potential of P4VPy forming the intermolecular hydrogen bonds with the proton-donor polymers, which are readily detected by means of infrared spectroscopy. Phenoxy is a typically self-associated polymer due to the presence of its pendent hydroxyls in the molecular backbone. The addition of P4VPy to phenoxy could give rise to the break of the self-associated hydrogen bonds of phenoxy, whereas the intermolecular hydrogen bonds will be formed between the chemically different chains. Shown in Fig. 4 are FTIR spectra of phenoxy and its blends with P4VPy in the region of 3100–3800 cm^{-1}. In this region, the spectroscopic bands are ascribed to the hydroxyl stretching vibration. For pure phenoxy, the very broad band was attributed to self-associated hydroxyls and the width of the band reflects the wide distribution of hydrogen-bonded hydroxyl stretching frequencies. For phenoxy/P4VPy blends, the broad hydrogen-bonded hydroxyl bands are observed to shift to lower frequencies with increasing P4VPy concentration. The shift of the hydrogen-bonded hydroxyl stretching bands to the lower frequencies is due to the breaking of –OH···OH hydrogen bonds and the formation of OH···N hydrogen bonds, which suggests that the intermolecular hydrogen bonding strength of the phenoxy/P4VPy blends is stronger than that of the self-association for pure phenoxy. In addition, it is noted that the newly appeared band at 3204 cm^{-1} upon mixing P4VPy to the system could be ascribed to the stretching vibration of hydrogen-bonded hydroxyls between phenoxy and P4VPy [25]. It should be pointed out that the shoulder bands centered at 3564 cm^{-1} are the stretching vibration of free hydroxyls. It is seen that the intensity of the free hydroxyl stretching bands decreases with increasing the content of P4VPy in the blends.

3.3. ^{13}C CP/MAS NMR spectroscopy

^{13}C CP/MAS spectra. The ^{13}C CP/MAS spectra of phenoxy, P4VPy, and their blends are shown in Fig. 5. The

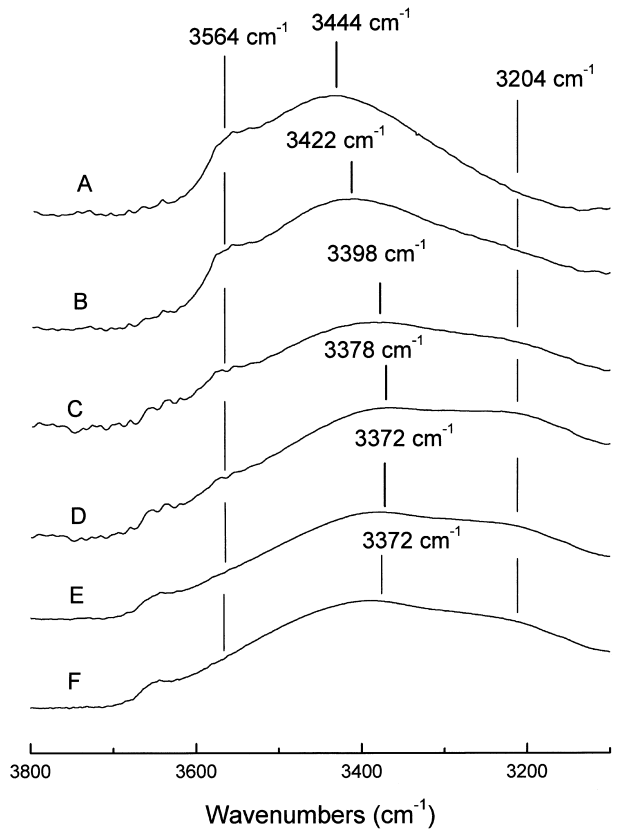

Fig. 4. FTIR spectra of phenoxy/P4VPy blends in the region of 3100–3800 cm^{-1}. (A) 100/0; (B) 90/10; (C) 70/3030; (D) 50/50; (E) 30/70; (F) 10/90.

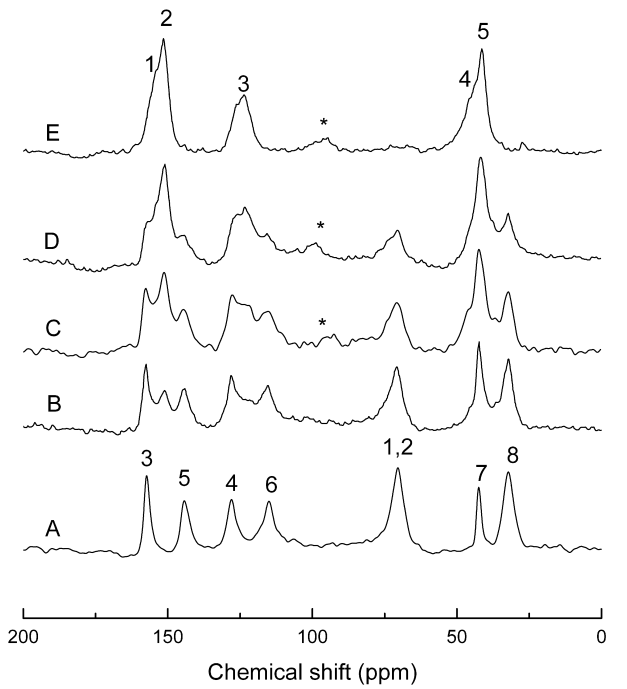

Fig. 5. ^{13}C CP/MAS NMR spectra of phenoxy/P4VPy blends. (A) 100/0; (B) 70/30; (C) 50/50; (D) 30/70; and (E) 0/100. Asterisks indicated spinning side bands.

seven peaks of phenoxy correspond to the methylene and the hydroxyl-substituted methylene carbons (C-1, C-2, 70 ppm), the methyl carbons (C-8, 33 ppm), the quaternary carbon (C-7, 43 ppm), and the other carbons in aromatic ring (C-3, 157 ppm; C-4, 128 ppm; C-5, 114 ppm, and C-6, 144 ppm). It is noted that there is an overlap of resonance peaks for methylene and hydroxyl-substituted methylene carbons (C-1 and C-2) in the ^{13}C CP/MAS NMR spectra of phenoxy.

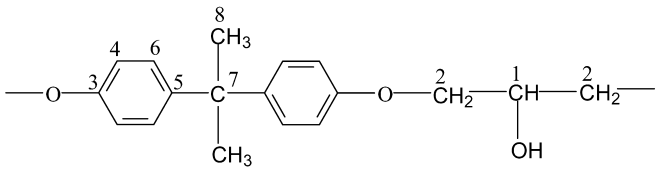

The above assignment of the ^{13}C CP/MAS spectrum of phenoxy was made by reference of the previous works [31, 32].

The assignment of the resonance lines of P4VPy were made as follows [33]:

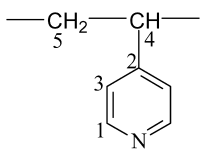

Compared with the ^{13}C CP/MAS spectra of the pure polymers, the ^{13}C CP/MAS spectra displayed some significant changes, especially for the resonance of the carbons involved in intermolecular (or intramolecular) hydrogen-bonding interactions. In the present paper, our attention is focused on the carbons of methylene (C-2, 70 ppm) and the hydroxyl-substituted methylene (C-1, 70 ppm) of phenoxy. Shown in Fig. 6 are the expanded ^{13}C CP/MAS spectra of phenoxy/P4VPy blends in the region of 60–84 ppm. It is noted that upon adding P4VPy to the system, the overlapped peaks become broader. There appear shoulders in the downfield in the resonance peaks and the intensity of shoulder peaks increased with increasing the P4VPy content. This change was attributed to the intermolecular specific interactions between phenoxy and P4VPy, i.e. the hydrogen bonding between the pendant hydroxyl of phenoxy and the nitrogen atom of P4VPy. The formation of intermolecular associations gave rise to the de-shielding effect of the electronic density of hydroxyl-substituted carbon; thus, the resonance of the carbons of methylene (C-2, 70 ppm) and the hydroxyl-substituted methylene (C-1, 70 ppm) of phenoxy tend to split since one component of the resonance peaks shifted downfield. Of course, the change of the chemical shift could also be relative to the change in the bond angle and intra-chain distance of the nearest neighbors. The spectral changes due to blending suggest intimate mixing of polymer chains of the two components. It should be pointed out that the chemical shifts of the resonance of other carbons were essentially unaffected by blending.

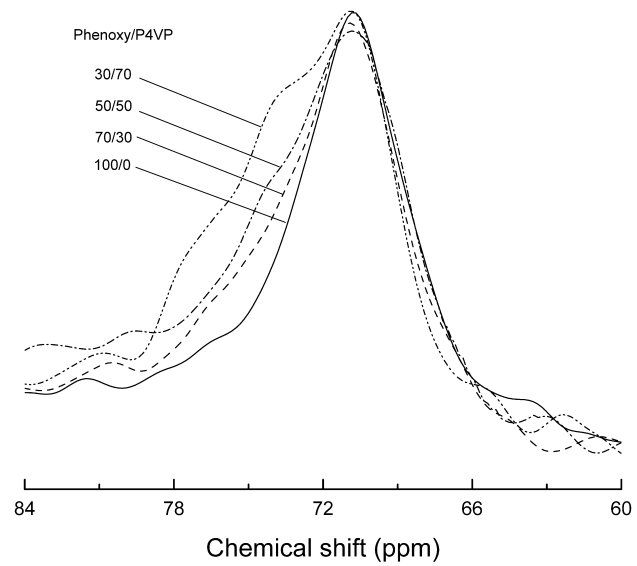

Fig. 6. ^{13}C CP/MAS NMR spectra of phenoxy/P4VPy blends in the region of 60–90 ppm.

$T_1(H)$ and $T_{1\rho}(H)$. To ascertain the homogeneity of the polymer blends, the relaxation behavior of protons was investigated. In polymer blends, the relaxation behavior of protons attached to different kinds of carbons greatly depends on the microscopic phase structures. In the miscible polymer blends on the molecular level, the protons of the chemically different chains are closely coupled and relaxed with an identical rate through spin-diffusion mechanism. The proton spin–lattice relaxation behaviors in the laboratory frame and the rotating frame are sensitive to the homogeneity resulting from short-range interacting dipole moments. Therefore, the T_1(H) and $T_{1\rho}$(H) values have been widely used to estimate the domain size. In this work, the dynamic relaxation experiment was conducted from the ^{13}C CP/MAS spectroscopy.

In the T_1 (H) experiment, an $180°-\tau-90°$ pulse sequence provides the T_1 relaxation times (Fig. 1(a)). The inverted magnetization, following the 180° pulse, decay through zero to return to its equilibrium state along H_0 with a characteristic time T_1(H). In the T_1 (H) experiment, the resonance intensities of phenoxy, P4VPy and their blends show the single-exponential increment as a function of delay time. The T_1(H) can be calculated according to the inversion-recovery mode for the experiment of relaxation times, and the following equation is employed to fit the curve with a single-exponential increment:

$$M(\tau) = M_\infty[1 - 2\exp(-\tau/T_1(\mathrm{H}))] \quad (3)$$

where M_∞ is the intensity of the resonance at $\tau \geq 5\ T_1$(H); T_1(H) is the relaxation time in the laboratory frame. Taking the natural logarithm of both sides, Eq. (3) gives:

$$\ln[M_\infty - M(\tau)] = -\tau/T_1(\mathrm{H}) + \ln(2M_\infty) \quad (4)$$

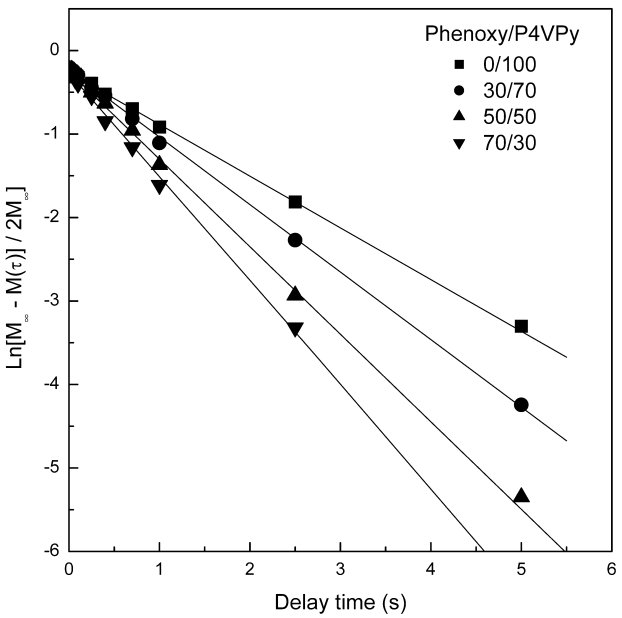

Fig. 7. Logarithmic plot of ^{13}C CP/MAS resonance intensity (at 151 ppm) vs. delay time for the blends to measure proton relaxation time for the laboratory frame.

The plots of $\ln[M_\infty - M(\tau)]$ vs. τ will yield T_1 (H) as shown in Fig. 7. It can be seen, that the experimental data were in a good agreement with those calculated from Eq. (4). From the slopes of the plots, T_1(H)s were obtained, and the results of T_1(H) for phenoxy, P4VPy and their blends are summarized in Table 1. The single values of T_1(H) was found intermediate between the relaxation times of the two pure components. These results indicate that fast spin diffusion carried out among all the protons in these blends, which averages out the whole relaxation process. Therefore, the blends are homogeneous on the scale where the spin diffusion occurs within the times of T_1(H). The mixing scale can be, therefore, estimated using the one-dimensional diffusion equation for the average diffusive path length [34–36]:

$$L = (6DT_i)^{1/2} \quad (5)$$

where D is the spin-diffusion coefficient depending on the average proton to proton distance as well as dipolar interaction; it has typically a value of the order of $10^{-16}\,m^2\,s^{-1}$. T_i is relaxation time (T_1(H) or $T_{1\rho}$(H)) according to the relaxation experiment. On the basis of T_1(H), it is believed that the two polymers are intimately mixed on a scale less than 20–30 nm. It should be pointed out that the quadrupolar nucleus with spin $I = 1$, ^{14}N (natural abundance of 99.63% is symmetrical in the pyridine ring of pure P4VPy. The formation of intermolecular hydrogen bonding through ^{14}N will confine the motion of the pyridine ring, and thus, the electric filed gradient of the nucleus, which is randomly modulated by the molecular motion and the bonding environment, is no longer zero in the blends. The fluctuating electric field gradient could provide a pathway for spin–lattice relaxation, so the spin–lattice relaxation process of protons could be more efficient by coupling to ^{14}N. The NMR result substantially support that of DSC, but the sensitivity of glass transition temperature approach (viz. DSC) to the dimensional level is only within this scale [1–3], whereas NMR can probe even smaller scale.

In order to examine the homogeneity of phenoxy/P4VPy blends at the molecular level, the indirect spin-diffusion process was further investigated by the spin–lattice relaxation experiments in the rotating frame $T_{1\rho}$(H). $T_{1\rho}$(H) is the characteristic time for M_0 to decay along the r.f. field H_1, and the magnetization is spin-locked along H_1 by pulse sequence of Fig. 1(b), a 90° pulse followed by a 90° pulse shift. In polymer blends the $T_{1\rho}$(H) values are influenced by the spin diffusion among protons of the component polymers. This efficiency, in turn, is dependent upon the short-range spatial proximity of chains. Therefore, the examination of $T_{1\rho}$(H) values provides information about the miscibility of blends on the segmental scale. In this measurement, the intensities of carbon resonance of phenoxy, P4VPy and their blends display single exponential decays as a function of delay time, and the $T_{1\rho}$(H) values were calculated according to the exponential function model:

$$M(\tau) = M_0 \exp(-\tau/T_{1\rho}) \quad (6)$$

Fig. 8 representatively shows the logarithmic plots of ^{13}C CP/MAS resonance intensity $M(\tau)$ vs. delay time for the selected carbon (at 151 ppm) of P4VPy and 70/30, 50/50, 30/70 phenoxy/P4VPy blends. It is noted that the fitting of

Table 1
Proton spin–lattice relaxation time T_1(H) (ms) of PH, P4VP and their blends in the laboratory frame

Phenoxy/P4VPy	Phenoxy, 157 ppm	P4VPy, 151 ppm	Phenoxy		P4VPy, 122 ppm	Phenoxy			P4VPy, 40 ppm	Phenoxy, 31 ppm
			143 ppm	127 ppm		114 ppm	69 ppm	42 ppm		
100/0	0.64		0.65	0.65		0.63	0.64	0.64		0.66
70/30	0.82	0.77	0.75	0.79	ND	0.72	0.80	0.82	ND	0.81
50/50	0.88	0.92	0.89	0.90	ND	0.88	0.92	0.95	ND	0.99
30/70	ND	1.23	ND	ND	1.12	ND	1.25	ND	1.19	1.12
0/100		1.61			1.51				1.71	

Accuracy is (±5%. ND: not detected due to low ratio of signal to noise or overlapping of resonance.

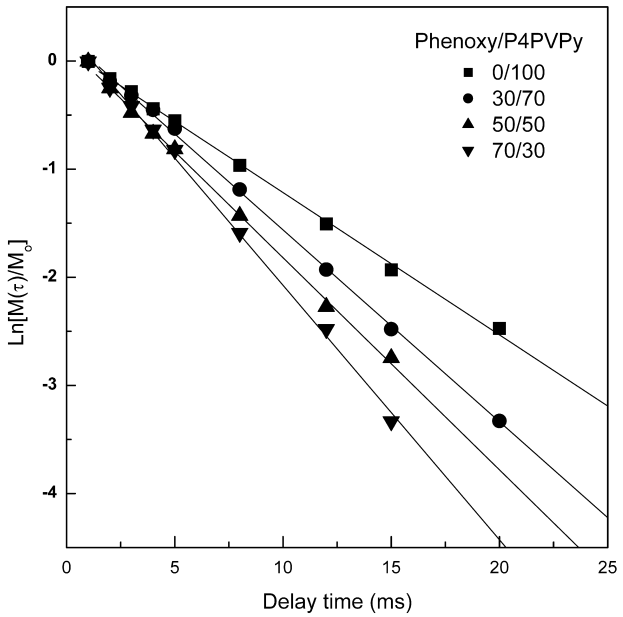

Fig. 8. Logarithmic plot of ^{13}C CP/MAS resonance intensity (at 151 ppm) vs. delay time for the blends to measure proton relaxation time for the rotating frame.

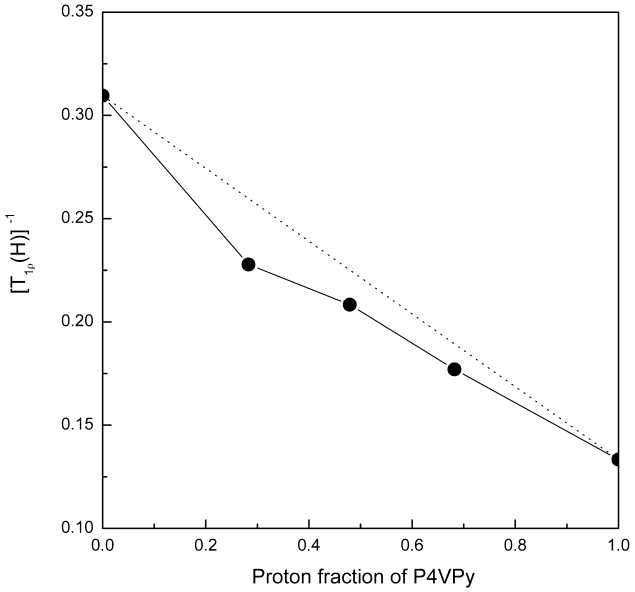

Fig. 9. Composition dependence of relaxation rates of phenoxy/P4VPy blends. (●) The experimentally obtained values; (- - -) the value predicted from Eq. (7).

the experimental data to a single exponential decay function is quite good. From the slope of the above plots, $T_{1\rho}$(H) was determined as summarized in Table 2. The single $T_{1\rho}$(H)s were obtained for the blends, which were intermediate between those of the two pure polymers. For the 70/30, 50/50, 30/70 blends, the $T_{1\rho}$(H) values of the resonance of all the carbons are identical. These results indicate that fast spin diffusion has been occurred among all the protons in these blends, thereby averaging out the whole relaxation process. It is judged that the blends are also homogeneous on the scale where the spin diffusion occurs within the $T_{1\rho}$(H) times. In view of $T_{1\rho}$(H)s, the average diffusive path length, viz. the domain size of the blends was calculated to be 20–30 Å.

Theoretically, if the motional state of each polymer component in a blend is not greatly changed by blending, then the average proton relaxation rate (the inverse of the relaxation time) of a homogeneous blend can be predicted by the model for the linear additivity of relaxation rates of the pure components [5,34]:

$$(T_1(\mathrm{H}))^{-1} = (N_\mathrm{A}/N)(T_1(\mathrm{H})_\mathrm{A})^{-1} + (N_\mathrm{B}/N)(T_1(\mathrm{H})_\mathrm{B})^{-1} \quad (7)$$

where $(T_1(\mathrm{H})_\mathrm{A})^{-1}$ and $(T_1(\mathrm{H})_\mathrm{B})^{-1}$ are the relaxation rates of pure components, N_A and N_B are the numbers of protons of the respective components and $N = N_\mathrm{A} + N_\mathrm{B}$. Fig. 9 shows the plot of $(T_{1\rho}(\mathrm{H}))^{-1}$ experimentally obtained and predicted by Eq. (7) as a function of blend composition. It is noted that the experimental values are less than those predicted from Eq. (7). Therefore, the blending of phenoxy and P4VPy seem to affect the segmental motional state of the components, which may reflect the stronger interaction between the two chains [8].

4. Conclusions

The blends of poly(hydroxyether of bisphenol A) (phenoxy) with poly(4-vinyl pyridine) (P4VPy) were

Table 2
Proton spin–lattice relaxation time T_1(H) (ms) of phenoxy, P4VP and their blends in the rotating frame

Phenoxy/P4VPy	Phenoxy, 157 ppm	P4VPy, 151 ppm	Phenoxy		P4VPy, 122 ppm	Phenoxy			P4VPy, 40 ppm	Phenoxy, 31 ppm
			143 ppm	127 ppm		114 ppm	69 ppm	42 ppm		
100/0	3.24		3.25	3.52		3.20	3.16	3.31		3.17
70/30	4.76	4.34	4.16	4.35	ND	4.35	4.34	4.54	ND	4.34
50/50	4.78	4.99	4.51	4.92	ND	4.68	4.76	5.04	ND	4.75
30/70	ND	5.26	ND	ND	5.88	ND	5.98	ND	5.55	5.56
0/100		7.69			7.60				7.30	

Accuracy is ±5%. ND: not detected due to low ratio of signal to noise or overlapping of resonance.

recognized to be miscible in terms of the behavior of single, composition-dependant glass transition temperatures (T_gs). The characteristic sigmoid T_g–composition relationship was reported in this work, suggesting the presence of the intermolecular specific interactions, which was in a good agreement with the studies of FTIR. The intermolecular hydrogen bonding was involved with pendant hydroxyl groups of phenoxy and nitrogen atoms in pyridine ring, and the strength of the intermolecular hydrogen bonding is much stronger than that of self-association in phenoxy. To examine the miscibility of the system at the molecular level, high-resolution ^{13}C CP/MAS together with the high-power DD NMR technique was employed. The chemical shift of hydroxyl-substituted methylene carbon resonance of P4VPy was observed to shift downfield in the ^{13}C CP/MAS spectra upon adding phenoxy to system, suggesting the formation of intermolecular hydrogen bonding. The proton spin–lattice relaxation time T_1(H) and the proton spin–lattice relaxation time in the rotating frame $T_{1\rho}$(H) were measured as a function of the blend composition. In light of the proton spin–lattice relaxation parameters, it is concluded that the phenoxy and P4VPy chains are intimately mixed on the scale of 20–30 Å.

Acknowledgements

This work was supported by RGC the Hong Kong Earmarked Grant for Research (No. RGC HKUST 6120/99P).

References

[1] Olabisi O, Robeson LM, Shaw MT. Polymer–polymer miscibility. New York: Academic Press; 1979.
[2] Utracki LA. Polymer alloy and blends. Munich: Hanser Publishers; 1989.
[3] Kaplan DS. J Appl Polym Sci 1976;20:2615.
[4] Coleman MM, Graf JF, Painter PC. Specific interaction and the miscibility of polymer blends. Lancaster, PA: Technomic Publishing Inc; 1991.
[5] Assink RA. Macromolecules 1978;11:1233.
[6] Cheung TTP, Gerstern BC, Ryan LM, Taylor RE, Dybowski. J Chem Phys 1980;73:6059.
[7] Cudby MEA, Packer KJ, Hendra PJ. Polym Commun 1984;25:303.
[8] Clauss J, Schmidt-Rohr K, Adam A, Boeffel C, Spiess HW. Macromolecules 1992;25:5208.
[9] Cai WZ, Schmidt-Rohr K, Egger E, Gerharz B, Spiess HW. Polymer 1993;34:267.
[10] Spiegel S, Schmidt-Rohr K, Boeffel C, Spiess HW. Polymer 1993;34:4566.
[11] Clauss J, Schmidt-Rohr K, Spiess HW. Acta Polym 1993;44:1.
[12] Zumbulyadis N. Phys Rev B 1983;33:6495.
[13] Clauss J, Schmidt-Rohr K, Spiess HW. Macromolecules 1992;25:3273.
[14] McBriety VJ, Douglass DC, Kwei TW. Macromolecules 1978;11:1265.
[15] Stejskal EO, Schaefer J, Sefcik MD, Mckay R. Macromolecules 1981;14:275.
[16] Dickinson LC, Yang H, Chu CW, Stein RS, Chien CW. Macromolecules 1987;20:1757.
[17] Grobelny J, Rice DM, Karasz FE, MacKnight WJ. Polym Commun 1990;31:86.
[18] Grobelny J, Rice DM, Karasz FE, MacKnight WJ. Macromolecules 1990;23:2139.
[19] Masson JF, Manley RSJ. Macromolecules 1992;25:589.
[20] Schenk W, Reichert D, Schneider H. Polymer 1990;31:329.
[21] Zhang X, Takagoshi K, Hikichi K. Polymer 1992;33:712.
[22] Feng H, Feng Z, Shen L. Polymer 1993;34:2516.
[23] Zhang X, Takegoshi K, Hichichi K. Macromolecules 1991;24:5756.
[24] Belfiore LA, Lutz TT, Cheng C. Solid state NMR of polymer. New York: Plenum Press; 1991. p. 145.
[25] Deilarduya AM, Eguiburu JL, Espi E, Iruin JJ, Fernandezberridi MJ. Makromol Chem 1993;194:501.
[26] Fox TG. Bull Am Phys Soc 1956;1:123.
[27] Gordon M, Taylor JS. J Appl Chem 1952;2:496.
[28] Couchman PR. Macromolecules 1978;11:1156.
[29] Kwei TK, Pearce EM, Pennacchia JR, Charton M. Macromolecules 1987;20:174.
[30] Kwei TK. J Polym Sci Polym Lett Ed 1984;22:307.
[31] Zheng S, Guo Q, Mi Y. J Polym Sci Part B: Polym Phys 1998;36:2291.
[32] Lau C, Zheng S, Zhong Z, Mi Y. Macromolecules 1998;31:7291.
[33] Wang J, Chang M-K, Mi Y. Polymer 2001;42:3087.
[34] Schaefer J, Slejskal EO. J Chem Soc 1976;98:1031.
[35] McBrierty VJ, Douglass DC. J Polym Sci, Macromol Rev 1981;16:295.
[36] McBrierty VJ, Douglass DC. Phys Rep 1980;63:61.